Performance-based design methodologies for geotechnical earthquake engineering

Steven L. Kramer

Abstract Performance-based design offers a number of advantages over historically common design approaches. As currently practiced, performance is most commonly evaluated in terms of system response, typically displacement-related, using traditional ground motion intensity measures defined at two or more discrete hazard levels. Such approaches do not necessarily allow all of the potential benefits of performance-based design to be realized. More recently, integral performance-based procedures that account for ground shaking hazards at all hazard levels have been developed. This paper reviews basic concepts of performance and different approaches to the implementation of performance-based design. An load and resistance factor-like methodology is described and illustrated with an example.

Keywords Performance-based design · Response · Seismic hazard · LRFD

1 Introduction

The use of performance-based concepts for seismic design has increased significantly over the past 10–15 ́years. The performance-based approach implies that structures and facilities can be designed and constructed in such a manner that their performance under anticipated seismic loading can be predicted with an acceptable degree of accuracy. The large uncertainties involved in characterizing anticipated ground motions, along with the significant uncertainties involved in predicting system response, physical damage, and losses have led most approaches to performance-based design to be formulated in probabilistic terms, although the probabilistic approach is not absolutely required, and not consistently used in current practice.

In practice, performance-based design of structures and facilities can be accomplished in many different ways. In this paper, the term "structures" will be used in a generic sense to describe systems that could include buildings and bridges, but also embankments, levees,

S. L. kramer (✉)
Department of Civil and Environmental Engineering, University of Washington, Seattle, WA, USA
e-mail: kramer@uw.edu

earth dams, natural slopes, foundations, etc. The paper will explore alternative approaches to performance-based design, discuss their implementation in practice, and show how the benefits of performance-based geotechnical design can be realized in a framework that most practitioners are already familiar with.

2 Historical approaches to geotechnical seismic design

For many years, geotechnical engineers based evaluations of "safety" on forces and stresses for both static and dynamic loading conditions. Such evaluations compare the shear stresses required to maintain equilibrium with the available shear strength of the soil, and express their results in terms of a factor of safety. A factor of safety greater than 1.0 is commonly taken to indicate a stable, or non-failure, condition. Conservatism has typically been provided through the specification of a design-level minimum factor of safety, which exceeds 1.0 by an amount that reflects uncertainty and consequences of failure, but also experience, precedent, convenience, and engineering judgment to varying degrees.

Early procedures for seismic design were simple extensions of the procedures used for static design. Beginning with analyses of retaining structures nearly 100 years ago (Mononobe and Matsuo 1929; Okabe 1926), the complex, transient, dynamic,inertial loads induced by earthquakes were replaced with simple static forces oriented in a manner that reduced stability in "pseudo-static" analyses. These pseudo-static forces increased the shear stress "demands" in the soil above those existing under static conditions and thereby reduced the pseudo-static factor of safety computed when all forces are considered. Recognizing that earthquakes are rare, that the demands they produce are transient in nature, and that force-based "failures" of very short duration were not necessarily damaging, pseudo-static designs have frequently been based on lower allowable factor of safety values than are used for static design.

Beginning with the development of the sliding block model (Newmark 1965), geotechnical engineers have worked to develop tools for predicting the permanent deformations of geotechnical structures subjected to earthquake loading. The ongoing development of stress-deformation analyses, implemented in finite element and finite difference computational platforms, has led to more and more powerful predictive potential, although data for validation of such models has lagged somewhat behind development of the models themselves. Recognizing the complexities involved with numerical predictions of earthquake-induced deformations, and the lack of full-scale, instrumented, field case histories against which to validate them, a number of simplified deformation models have been developed and used in practice. For foundations, the development of macro-element models (e.g., Nova and Montrasio 1991; Paolucci 1997; Cremer et al. 2001, 2002; Chatzigogos et al. 2011; Correia et al. 2012) have allowed efficient computation of nonlinear inelastic response of foundations subjected to multi-dimensional dynamic loading. Makdisi and Seed (1978), for example, performed sliding block analyses to develop a correlation between peak ground acceleration and the expected permanent deformations of embankment dams. The proposed model was properly described as producing uncertain deformation estimates, but the Makdisi-Seed average curves have been widely and continuously used for deterministic estimates of slope displacement since they were published. A number of empirical and semi-empirical models for estimation of deformations have been developed. Empirical procedures for estimation of lateral spreading displacement (e.g., Bartlett and Youd 1992; Youd et al. 2002) are based on interpretation of lateral spreading case histories.

3 Seismic performance

The term "performance" can mean different things to different people involved in the seismic design process. Ground displacement can be a good measure of performance to the designer of an earth dam. To a structural engineer, a measure of response such as interstory drift would be a good descriptor of building performance. To an estimator preparing a bid for repairs, measures of physical damage such as crack width and spacing could be more useful measures of performance. Finally, to an owner, the economic loss associated with earthquake damage could be the best measure of performance.

3.1 System response

Structures, whether comprised of steel, concrete, or soil, have mass and flexibility, and therefore respond more strongly at some frequencies than others. They exhibit generally linear behavior at very low levels of loading but can become highly nonlinear and inelastic at higher levels of shaking. Response can be expressed in terms of forces and stresses or displacements and strains, and are frequently characterized by engineering demand parameters, or *EDP*s. When the level of response is too high, damage can occur. In order to accurately predict the damage associated with structural response, it is necessary to identify the measures of response that are most closely related to damage, and to be able to predict the response caused by earthquake ground motion.
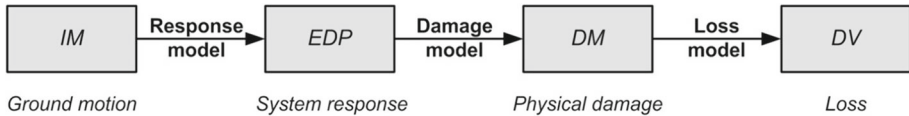
3.2 Physical damage

The response of a structure may or may not result in physical damage depending on the structure's capacity to resist damage. The capacity may be viewed as a level of response beyond which some level of physical damage can be expected to occur. Many different types of damage can occur during an earthquake—some can be related to the structure itself, some to physical systems within the structure, and some to the contents of the structures. In order to predict the losses associated with various forms of physical damage, it is necessary to identify the specific form(s) of physical damage, quantified by damage measures, or *DM*s, that contribute most strongly to the losses of interest, and to be able to predict the physical damage associated with the response of the system of interest.

3.3 Losses

Physical damage to structures and their contents result in losses. Losses can have many components—deaths and injuries, repair and replacement costs, and loss of utility for extended periods of time. Decisions regarding risk reduction through retrofitting, insurance protection, etc. are usually made on the basis of expected losses, so those losses are often characterized by decision variables, or *DV*s.

3.4 Predicting performance

A complete prediction of performance requires prediction of the response, damage, and loss associated with one or more specific levels of ground shaking. This process can be illustrated schematically as shown in Fig. 1. A response model, which can range from an empirical algebraic equation to a detailed nonlinear finite element model, is used to predict the response

Fig. 1 Schematic illustration of process by which response, damage, and loss are predicted

of a soil-structure system to earthquake shaking. A damage model is used to predict physical damage from response levels. The damage model may be analytical or heuristic in nature. Finally, losses are predicted from damage by a loss model. The loss model may be a relatively straightforward combination of repair quantities and unit costs, or a complex financial model that considers indirect losses, future interest rates, etc.

4 Performance-based seismic design

Early efforts at seismic design were scenario-based, i.e., based on the identification of one or more "design earthquakes" (e.g., maximum credible and maximum probable earthquakes) typically specified by source, magnitude, and distance. The ground motions associated with the design earthquakes were estimated deterministically, initially by heuristic specification of ground acceleration, but later using median values from early attenuation relationships. These median values generally neglected the uncertainty inherent in ground motion estimation.

An important advance in seismic design came in the late 1970s with the publication of the ATC-3-06 (Applied Technology Council 1978) report. ATC-3-06 built on the probabilistic seismic hazard analysis concepts of Cornell (1968) and the mapping work of Algermissen and Perkins (1976) to express design seismic loading in a probabilistic manner. ATC-3-06 recommended that design be based on a single level of ground shaking—that with a 10 percent probability of exceedance in a 50-years period, i.e., a 475-years return period. For structures, ATC-3-06 provided guidance for the allowance of inelastic behavior of components through the provision of ductility, and based performance on the relationship between estimated and allowable interstory drifts. The allowable story drifts were presented for four seismic performance categories in three seismic use groups. Thus, the use of deformation-based response and capacity measures as metrics of performance was introduced.

4.1 Discrete hazard level approach

More recent performance objectives are expressions of the acceptable risk of experiencing different levels of damage or loss. Owners are typically willing to accept a higher risk of low levels of damage/loss than high levels, and may define different acceptable likelihoods for different levels. The first document widely recognized as establishing such procedures for performance-based design of new structures was the Vision 2000 report (SEAOC 1995). The Vision 2000 report described the general levels of damage to various building components and provided allowable inter-story drift limits associated with the four performance levels (fully operational, operational, life safe, and near collapse). Fully operational performance was expected for frequently levels of shaking, which were taken as having a return period of 43 years. Operational, life safe, and near collapse performance levels were expected for motions with return periods of 72, 475, and 975 years, respectively. These limits were expressed deterministically but were intended to be conservative; the degree of conservatism,

for example in terms of the actual return period at which the different performance levels would be reached, is not known.

4.2 Integral hazard level approach

The Pacific Earthquake Engineering Research Center (PEER) has proposed a framework for PBEE (Cornell and Krawinkler 2000; Deierlein et al. 2003). The framework makes use of the previously described notation, and recognizes the fact that *IM*s, *EDP*s, *DM*s, and *DV*s, as well as the relationships between them, are all uncertain. The PEER framework is encapsulated in a "framing equation" formally presented in its most general form as

$$\lambda(\boldsymbol{DV}) = \int \int \int G(\boldsymbol{DV}|\boldsymbol{DM}) \, |dG(\boldsymbol{DM}|\boldsymbol{EDP})| \, |dG(\boldsymbol{EDP}|\boldsymbol{IM})| \, |d\lambda(\boldsymbol{IM})| \qquad (1)$$

In Eq. (1), $G(a|b)$ denotes a complementary cumulative distribution function (CCDF) for a conditioned upon b (the absolute value of the derivative of which is the probability density function for a continuous random variable) and the bold type denotes vector quantities. From left to right, the three CCDFs result from loss, damage, and response models; the final term, $d\lambda$ (*IM*) is obtained from the mean seismic hazard curve; uncertainty in the position of the *IM* hazard curve itself is not considered. The framing equation implicitly assumes that the quantities used to describe *IM, EDP*, and *DM* are each capable of predicting *EDP, DM*, and *DV*, respectively.

The framing equation allows calculation of loss hazard (i.e., the mean annual rate of exceeding various levels of loss) by integrating over all levels of ground motion, response, and damage with the contributions of each of those variables weighted by their relative likelihoods of occurrence. The computed loss hazard can be viewed as the weighted average of all possible earthquake, ground motion, response, damage, and loss scenarios. It can account not only for location-dependent differences in tectonic environment but also for local differences in construction quality (as evidenced by capacities to resist damage), repair costs, and local indirect costs. It can therefore allow a uniform, objective, and consistent estimate of losses in different geographic regions.

This triple integral can be solved directly only for an idealized set of conditions, so it is solved numerically for most practical problems. When all variables are continuous, the numerical integration can be accomplished (assuming scalar parameters for simplicity) as

$$\lambda_{DV}(dv) = \sum_{k=1}^{N_{DM}} \sum_{j=1}^{N_{EDP}} \sum_{i=1}^{N_{IM}} P[DV > dv|DM = dm_k] \times P[DM > dm_k|EDP = edp_j]$$
$$\times P[EDP > edp_j|IM = im_i]\Delta\lambda_{IM}(im_i) \qquad (2)$$

where P[a|b] describes the probability of a given b, and where N_{DM}, N_{EDP}, and N_{IM} are the number of increments of *DM*, *EDP*, and *IM*, respectively. The variable b is considered to be an efficient predictor of a if the uncertainty in $a|b$ is low; b would be a sufficient predictor of a if the uncertainty in $a|b$ is not reduced by additional predictive variables.

The PEER framework has the useful benefit of being modular. The discretized framing equation (Eq. 2) can be broken down into a series of components, e.g.,

$$\lambda_{EDP}(edp) = \sum_{i=1}^{N_{IM}} P[EDP > edp|IM = im_i]\Delta\lambda_{IM}(im_i) \qquad (3a)$$

$$\lambda_{DM}(dm) = \sum_{j=1}^{N_{EDP}} P[DM > dm | EDP = edp_j] \Delta \lambda_{EDP}(edp_j) \tag{3b}$$

$$\lambda_{DV}(dv) = \sum_{k=1}^{N_{DM}} P[DV > dv | DM = dm_k] \Delta \lambda_{DM}(dm_k) \tag{3c}$$

which means that hazard curves can be computed for *EDP*, *DM*, and *DV* and interpreted in the same manner as the more familiar seismic hazard curve (for *IM*) produced by a PSHA.

Many seismic hazard curves are nearly linear on a log–log plot, at least over significant ranges of ground motion intensity (Department of Energy 1994; Luco and Cornell 1998), which implies a power law relationship between mean annual rate of exceedance and *IM* that can be expressed as

$$\lambda_{IM}(im) = k_0(IM)^{-k} \tag{4}$$

In this expression, k_0 is the value of $\lambda_{IM}(im = 1)$ and k is the slope of the seismic hazard curve (in log–log space, in which Eq. (4) plots as a straight line). If the response model is also assumed to be of power law form,

$$EDP = a(IM)^b \tag{5}$$

with lognormal response model dispersion, $\sigma_{\ln EDP|IM}$, the resulting *EDP* hazard curve can be expressed as

$$\lambda_{EDP}(edp) = k_0 \left[\left(\frac{edp}{a} \right)^{1/b} \right]^{-k} \exp \left[\frac{k^2}{2b^2} \sigma^2_{\ln EDP|IM} \right] \tag{6}$$

This equation describes the mean annual rate of exceeding some level of response, *EDP* = *edp*, given the seismic hazard curve, which is the result of a probabilistic seismic hazard analysis, and a probabilistic response model. It therefore considers *all* possible values of *IM* rather than only those corresponding to the small integer number of return periods considered in the discrete hazard approach. Equation (6) is composed of two parts, the first of which is a function of *edp* and the constants (k_0, k, a, b) that describe the mean hazard curve and the median *EDP–IM* relationship (i.e., the response model). The second part depends on the slopes of the hazard curve and median response model relationship and, most significantly, on the uncertainty in the response model. The second term can be viewed as an "uncertainty multiplier" since its value is 1.0 when there is no uncertainty and becomes progressively greater than 1.0 as the response model uncertainty increases. This result shows that the mean annual rate of exceedance of a particular *EDP* value increases with increasing uncertainty. Put another way, the *EDP* value corresponding to a given mean annual rate of exceedance (or return period) increases with increasing response model uncertainty.

5 Performance-based design methodologies

Performance-based design can be implemented into engineering practice in a number of different ways. Different implementation methodologies must address two main matters—the manner in which earthquake loading is specified and the manner in which performance is evaluated. The design process involves an iterative series of performance evaluations after which the computed performance is compared with the performance objectives, and

the design is modified until all performance objectives have been met. The performance evaluations may be based on measures of response, damage, or loss.

In the simplest approach, PBD can be implemented at the response level, i.e., by specifying performance in terms of *EDP* values at different response hazard levels (or response return periods). In this approach, physical damage and loss must be inferred from the computed response. This inference may be guided by judgment and experience, but must be recognized as leading to uncertain loss estimates. An intermediate approach would be to specify performance in terms of damage limit states, which involves the explicit comparison of predicted and allowable damage; this approach would involve prediction of *DM*s with consideration of response and damage model uncertainties. Ledezma and Bray (2010) analyzed a five-span bridge typical of that designed by the California Department of Transportation supported by piles extending through liquefiable soils that were susceptible to lateral spreading. Approach embankment displacements were computed using the procedure of Bray and Travasarou (2007) and pile–soil interaction was accounted for using a pile pinning analysis. Five discrete damage states (none, small, moderate, large, and collapse) were defined on the basis of pile response. Loss would still need to be inferred, but inferring loss from specific damage levels involves less uncertainty than inferring it from specific response levels. The most complete level of implementation would be to involve the definition of performance in terms of losses (*DV*s), which would involve explicitly modeling response, damage, and loss with consideration of the uncertainties inherent in each. While requiring more information and more effort, this approach would provide the most accurate (i.e., least uncertain) estimate of loss. Iai et al. (2008) described the design of a caisson quay wall in 15 m of water resting on a rubble fill underlain by alluvial clay, and retaining liquefiable soil. Using a series of parametric (finite element) response analyses, fragility curves for one damage state were developed. Assigning a repair cost of 1M yen/m of wall length and considering the construction costs for different improvement options, life-cycle costs for each of five improvement options could be calculated. Towhata et al. (2009) described an example of performance-based design of the widening of an expressway embankment based on life-cycle cost concepts. Rix (2009) extended the life-cycle cost approach to include time-value-of-money effects and the dispersion of estimated loss, and computed combinations of the mean and standard deviation of expected loss. With such data, owners with different risk tolerances could choose between strategies with low mean loss but high uncertainty or higher mean loss with lower uncertainty.

Kramer (2011) recently presented the results of a brief and informal online survey of practicing engineers in North America on their current seismic design practices. When asked how they measured performance, the responses indicated a strong emphasis on measures of deformation (displacement, rotation, strain, etc.) as indicators of performance, with multiple respondents indicating that they considered performance-based design to be synonymous with deformation-based design. The practitioners listed several impediments to the increased use of performance-based design in engineering practice. Many of the respondents felt that engineers, owners, and regulators were not sufficiently convinced of the benefits of the performance-based approach, and not sufficiently educated about the procedures used to develop a performance-based design. Respondents also felt that improved, validated tools for nonlinear response analysis, including soil-structure interaction, were required to advance the use of performance-based design. A number of respondents felt that proficiency with the probabilistic concepts that underlie performance-based design was lacking, and that improved education and tools for probabilistic analysis would be beneficial. Other respondents believed that regulators and code-writing bodies should take the lead in promoting performance-based design by allowing (or requiring) its use in appropriate situations and working toward performance-based codes for common structures. Finally, the lack of fre-

quent interaction between geotechnical engineers, the rest of the design team, and owners was listed as a significant impediment by a number of survey respondents.

For very large projects, the complete PBEE methodology may be too time-consuming for design iterations. In such cases, conventional deterministic procedures may be used to narrow down the range of component design alternatives with the PBEE methodology subsequently used to complete the design process.

5.1 Response-level implementation

If the profession's belief is that performance is currently best evaluated at the response level, procedures for performance-based design must be implemented at the response level. A number of response-level performance evaluations have been reported in the literature. Biondi et al. (2009) described a performance-based procedure for gravity retaining walls in which a Richards-Elms Richards and Elms (1979) type procedure was used to estimate lateral wall displacements, which were then related to a limiting yield coefficient. A factor of safety defined using this yield coefficient and the yield coefficient corresponding to the allowable displacement served as an indicator of whether the allowable displacement was exceeded. Sunasaka et al. (2009) summarized the performance-based design of a pile-supported platform and seawall adjacent to a reclaimed island at the Tokyo International Airport. Finite element soil-structure analyses were used to compute system deformations, including the relative displacement between the seawall and the platform. Pile performance was checked by comparing computed pile curvatures to the allowable curvatures, which were those that would cause yielding of the piles.

A response-level implementation using the PEER framework would allow evaluation of the mean annual rate of exceedance (or return period) of various levels of response. By combining the results of a PSHA with a probabilistic response model, this approach can provide a consistent and objective evaluation of seismic response hazards in different tectonic environments.

Performance-based procedures for liquefaction hazard evaluation have been developed (Marrone et al. 2003; Kramer and Mayfield 2005, 2007; Juang et al. 2008), permanent slope displacements (Travasarou et al. 2004; Rathje and Saygili 2008), and pile foundation response (Cubrinovsky and Bradley 2009). Kramer and Mayfield (2007) described a performance-based procedure for evaluating liquefaction potential that resulted in factor of safety hazard curves that account for all *PGA* levels and all magnitudes that contribute to those *PGA* level. Rathje and Saygili (2008) described a probabilistic seismic displacement analysis using a regression equation for displacement calibrated to approximate the results of sliding block analyses. Using *PGA* as a scalar *IM*, a hazard curve for slope displacement could be obtained. Cubrinovsky and Bradley (2009) used the integral response approach to develop pile head displacement hazard curves before and after proposed strengthening of a bridge in Christchurch, New Zealand. Basing design on a particular return period for liquefaction, as suggested by Kramer et al. (2006) or for slope displacement or pile head displacement would provide more uniform performance than the current process of basing such evaluations on deterministic factors of safety computed for a small number of discrete ground motion hazard levels.

6 Design of foundations

The design of foundations for buildings, bridges, and other structures is strongly influenced by seismic considerations in many regions of the world. In the United States, for example, bridge foundations are typically designed using load and resistance factor (LRFD) design. In LRFD,
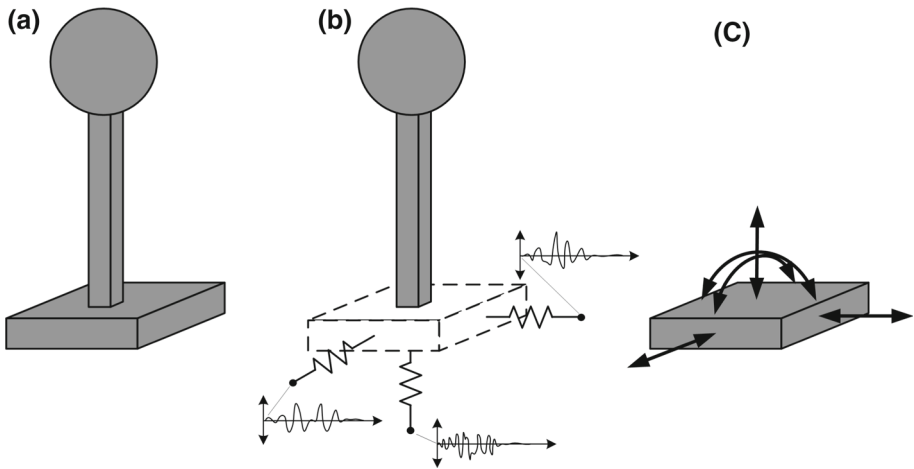
Fig. 2 Schematic illustration of decoupled approach: **a** soil-foundation-structure system, **b** structural system with input motions applied through elements of appropriate impedance, **c** forces computed from structural system applied to foundation

uncertainties in load and resistances are characterized and used to develop factors by which nominal loads and resistances are multiplied to produce factored loads and resistances that, when equal, correspond to a particular probability of failure. A successful design, therefore, will be one in which the factored resistance exceeds the factored load.

A more general description of seismic performance can be obtained by consideration of demands and capacities. In a force-based evaluation, forces can act as demands and resistance as capacities. However, in a displacement-based evaluation, demands can be represented by the displacement(s) of a structure excited by earthquake loads, and allowable displacement(s) can be taken to represent the capacity of the structure to tolerate displacement. Thus, reference can be made to force or displacement demand and to load or displacement capacity.

Ideally, the response of a soil-foundation-structure system to earthquake shaking would be predicted by coupled nonlinear analyses of the complete soil-foundation-structure system. In order to investigate general procedures for seismic design of foundations, however, the infinite number of possible structure, site, and foundation configurations must be recognized. In order to avoid developing procedures that are excessively structure/site/foundation-dependent, the problem can be decoupled using the type of decoupled substructure analysis that is commonly used in soil-structure interaction analysis. In the decoupled approach, a soil-foundation-structure model (Fig. 2a) is broken down into two components. A structural model (Fig. 2b) supported by appropriate springs and dashpots is subjected to three-dimensional shaking applied through the spring/dashpot elements. The structure responds dynamically, producing forces and overturning moments that act on the foundation. The connection between the structure and the foundation, therefore, is subjected to three orthogonal forces, and two orthogonal overturning moments; torsion of an individual foundation is usually not significant. These loading histories are computed and saved for use in a second analysis (Fig. 2c), which is performed on a soil-foundation model that is excited by the loading histories from the first analysis. This loading causes displacement and rotation of the footing, which are also recorded. The load measure is a term that characterizes the nature of the dynamic load—the peak (absolute) dynamic load would be a simple and useful *LM*. The displacements and rotations can be represented by the *EDP*, a five-component vector. Peak or permanent values of displacement or rotation are useful potential *EDP*s.

6.1 Characterization of ground motion intensity

Characterization of earthquake loading first requires selection of one or more ground motion intensity measures. The selection, however, must be made with consideration of the system response of greatest interest. Ground motion intensity measures should ideally be predictable, efficient, and sufficient.

Intensity measure predictability refers to the uncertainty with which an *IM* can be predicted for a given earthquake scenario; this uncertainty is characterized by the standard error term in the ground motion prediction equation (GMPE) for that *IM*. Different *IM*s have been shown to have different levels of predictability. For structures, the use of spectral acceleration at the fundamental period as a scalar intensity measure is common.

6.2 Characterization of demand

Demand can be characterized as a level of response induced in a structure by earthquake loading. It can be expressed in terms of forces and/or moments or in terms of displacements and/or rotations. In a force-based approach, peak dynamic forces/moments are most commonly used to characterize demand. In some cases, these values may be normalized by a reference force/moment to produce a dimensionless load ratio. If the reference force/moment is taken as the failure load, a load ratio of 1.0 would imply failure. In a displacement-based approach, peak or permanent displacements/rotations can be used as displacement demands. For buildings, which are normally subjected to predominantly vertical static loads, permanent displacements/rotations are generally small so peak displacements/rotations provide a better indication of demand. Bridges, on the other hand, are frequently constructed on sloping ground that imposes significant horizontal static loads and/or overturning moments on foundations. In such cases, permanent displacements/rotations may be better measures of demand than peak values.

Seismic demands can be estimated in a number of ways ranging from simplified approximations to empirical methods to detailed dynamic analyses. Force demands can be computed by modal superposition for linear systems or nonlinear analysis for nonlinear systems, or can be estimated using code-based procedures. Displacement demands can be obtained from similar types of analyses. The uncertainties in displacement demands, while seldom rigorously documented, are generally considered to be significantly higher than uncertainties in force demands.

6.3 Characterization of capacity

To date, much more effort in geotechnical earthquake engineering has been placed on the prediction of response than on the prediction of damage given response. The ability of buildings, bridges, and other structures to tolerate ground movement has not received a great deal of research attention, and remains somewhat poorly understood. Bird et al. (2005) used basic mechanical principles to evaluate damage to reinforced concrete frame buildings from differential horizontal and vertical ground movements. Considering uncertainties in input parameters, fragility curves for damage limit states (Fig. 3) were obtained. Bird et al. (2005) used these damage models to compare damage scenarios with and without consideration of ground failure-induced damage at a liquefiable site. The fragility curves suggest limit state uncertainties of $\sigma_{\ln LS|\Delta} \approx 0.8$ for horizontal displacement and $\sigma_{\ln LS|\Delta} \approx 0.6$ for vertical displacement.
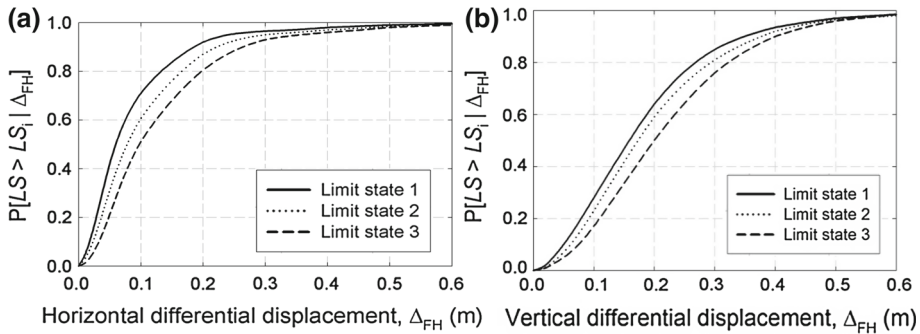
Fig. 3 Fragility curves for specific class of reinforced concrete building (after Bird et al. 2005). Limit states *1*, *2*, and *3* mark boundaries between slight and moderate, moderate and extensive, and extensive and complete damage, respectively

In current practice, capacities are effectively defined as limiting response levels beyond which various levels of damage and loss are assumed to occur. These limiting values are usually specified on the basis of a project-specific structural analysis that may or may not account for project-specific soil conditions, and usually represent a conservative, but deterministic, estimate of limiting response. The level of conservatism in the allowable response value is not standardized or quantified, and likely varies from one designer to another.

In reality, a limiting response level should be recognized as being uncertain, and the level of uncertainty as depending on the procedure(s) used to define it. Rather than characterizing allowable response conservatively and deterministically, it is possible to characterize the distribution of allowable response as accurately and objectively as possible and to include its uncertainty in the performance evaluation.

7 An LRFD-like performance-based design methodology

The practice of foundation design is increasingly being accomplished using load and resistance factor design (LRFD) techniques. LRFD recognizes that uncertainties in loads and resistances are different and characterizes them separately. Factored loads, i.e., the products of load factors and nominal loads are required to be less than factored resistances, which are the products of resistance factors and nominal resistances. In concept, load and resistance factors are calibrated to achieve some desired, time-invariant probability of failure (capacity exceedance). In practice, however, calibration is often based on a target of consistency with prior allowable stress design.

In seismic design, strong demands result from infrequent earthquake loading and therefore cannot be treated as time-invariant. At a given site, the value of a ground motion intensity measure that a particular structure may be subjected to depends on earthquake source, path, and site effects, all of which are highly uncertain. These uncertainties are generally accommodated through probabilistic seismic hazard analyses, which predict the rates at which various levels of ground shaking will occur by considering all possible sources, magnitude, and distances, and by considering ground motion uncertainty. The design level of ground motion is generally expressed in terms of a design *IM*, i.e., one with a particular mean annual rate of exceedance, or return period. This ground motion level is generally taken as a nominal level that is used to compute dynamic response.

In much the same way that loads and resistances can be factored for force-based design of time-invariant systems, response and capacity factors can be factored for seismic design. Jalayer (2003) and Cornell et al. (2002) laid out a procedure for structural design that can be adapted for foundation design. This leads to the possibility of two different approaches to seismic LRFD—one based on forces and the other on displacements.

7.1 Force-based approach

As previously discussed, seismic design can be based on loads or displacements, and both load and displacement response can be computed in the previously described decoupled analyses. In a force-based approach, the load measure would be a function of the intensity measure, i.e., $\mathbf{LM} = f(\mathbf{IM})$. Since that function would have some uncertainty, the PEER framework could be used to compute

$$\lambda_{LM}(lm) = \int G(\mathbf{LM}|\mathbf{IM}) |d\lambda(\mathbf{IM})| \approx \sum_{i=1}^{N_{IM}} P[LM > lm|IM = im_i]\Delta\lambda_{IM}(im_i) \quad (7)$$

If the *IM* hazard curve is defined as in Eq. (4) and *LM* is a lognormally distributed power law function of *IM*, i.e., $LM = aIM^b$, a closed-form expression for λ_{LM} can be derived as

$$\lambda_{LM}(lm) = k_0 \left[\left(\frac{lm}{a} \right)^{1/b} \right]^{-k} \exp\left[\frac{k^2}{2b^2}\beta_L^2 \right] \quad (8)$$

where $\beta_L = \sigma_{\ln LM|IM}$ represents the dispersion in loading given the intensity measure. Equation (8) should be noted as being analogous to Eq. (6).

7.1.1 Load capacity exceedance rate

Accounting for the fact that the foundation capacity is also uncertain, a hazard curve for the limit state, $LS = LM \geq C = c$, can be expressed as

$$\lambda_{LS} = \int_0^\infty \lambda_{LM}(c) f_C(c) dc \quad (9)$$

Equation (9) can be integrated numerically to compute the mean annual rate of limit state exceedance. The computed rates depend on the *IM* hazard curve, the (probabilistic) relationship between *IM* and *LM*, and the uncertainty in displacement capacity.

Under the assumptions of the closed-form solution and using Eqs. (8) and (9), the rate at which the load capacity, $C = c$, would be exceeded is

$$\lambda_{LS} = \int_0^\infty k_0 \left[\left(\frac{c}{a} \right)^{1/b} \right]^{-k} \exp\left[\frac{1}{2}\frac{k^2}{b^2}\beta_L^2 \right] f_C(c) dc \quad (10)$$

Letting $\hat{C}$ represent the median capacity and the dispersion in capacity, $\beta_C = \sigma_{lnC}$, Eq. (10) becomes

$$\lambda_{LS} = k_o \left(\frac{\hat{C}}{a} \right)^{-k/b} \exp\left[\frac{1}{2}\frac{k^2}{b^2}(\beta_L^2 + \beta_C^2) \right] \quad (11)$$

Fig. 4 Schematic illustration of load measure hazard curves for cases of no uncertainty, uncertainty in load given ground motion intensity, and uncertainties in load given ground motion intensity and capacity
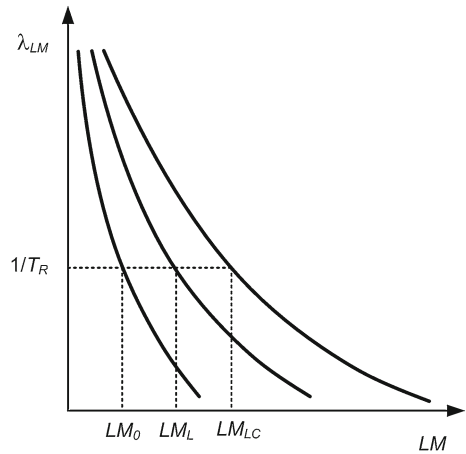
The mean annual rate of load capacity exceedance, therefore, can be seen to increase with increasing uncertainty in capacity as well as uncertainty in loading.

The closed-form expressions for mean annual rate of exceedance can each be solved for the value of LM corresponding to a particular mean annual rate of exceedance. These values, for the cases of (a) zero uncertainty in response and capacity ($\beta_L = \beta_C = 0$), (b) uncertain response but zero uncertainty in capacity ($\beta_L > 0$, $\beta_C = 0$), and (c) uncertain response and capacity ($\beta_L > 0$, $\beta_C > 0$), can be written as

$$LM_0 = a \left(\frac{\lambda_{LM}}{k_0} \right)^{b/k} \tag{12}$$

$$LM_L = a \left(\frac{\lambda_{LM}}{k_0} \right)^{b/k} \exp \left[\frac{k}{2b} \beta_L^2 \right] \tag{13}$$

$$LM_{LC} = a \left(\frac{\lambda_{LM}}{k_0} \right)^{b/k} \exp \left[\frac{k}{2b} \left(\beta_L^2 + \beta_C^2 \right) \right] \tag{14}$$

The values of LM_0, LM_L, and LM_{LC} are illustrated schematically in Fig. 4. As would be expected, the values of LM at a particular hazard level increase with increasing uncertainty.

7.1.2 Load and resistance factors

In static LRFD, a nominal load is multiplied by a load factor and a nominal capacity is multiplied by a resistance factor to achieve some desired probability of failure (capacity exceedance) or reliability index. For seismic LRFD, nominal loads and capacities should be multiplied by load and resistance factors to achieve some desired mean annual rate (or return period) of capacity exceedance. Taking the nominal load as the zero-uncertainty (median) load measure, LM_0, and the nominal capacity as the median capacity, $\hat{C}$, the load factor, LF, and resistance factor, RF, for a particular return period would be given by

$$LF = \frac{LM_L}{LM_0} \tag{15a}$$

and

$$RF = \frac{LM_L}{LM_{LC}} \tag{15b}$$

With this approach, a design that satisfies the condition

$$LF \cdot \hat{L}_p \leq RF \cdot \hat{C} \tag{16}$$

where $\hat{L}_p$ is the median load measure corresponding to $\lambda_{LM} = p$ and $\hat{C}$ is the median capacity would result in a mean annual rate of limit state exceedance equal to that corresponding to $\hat{L}$ and $\hat{C}$.

Substituting Eqs. (12)–(14) into Eq. (15), the closed-form load and resistance factors can be expressed as

$$LF = \exp\left[\frac{1}{2}\frac{k}{b}\beta_L^2\right] \tag{17a}$$

and

$$RF = \exp\left[-\frac{1}{2}\frac{k}{b}\beta_C^2\right] \tag{17b}$$

Note that, under the assumptions of the closed-form solution, the load and resistance factors are constants, i.e., they do not vary with return period.

7.2 Displacement-based approach

In a displacement-based framework, the uncertain relationships between *IM* and *LM*, and between *LM* and *EDP*, can also be accommodated by the PEER integral

$$\lambda_{EDP}(\textbf{\textit{edp}}) = \int \int G(\textbf{\textit{EDP}}|\textbf{\textit{LM}}) \,|dG(\textbf{\textit{LM}}|\textbf{\textit{IM}})| \,|d\lambda(\textbf{\textit{IM}})| \tag{18}$$

If the *LM*–*EDP* relationship is assumed to be governed by a power law with lognormally distributed *EDP*s, i.e. $EDP = dLM^e$, a closed-form expression for λ_{EDP} can be derived as

$$\lambda_{EDP}(edp) = k_0 \left[\frac{1}{a}\left(\frac{edp}{d}\right)^{1/e}\right]^{-k/b} \exp\left[\frac{k^2}{2b^2e^2}\left(e\beta_L^2 + \beta_R^2\right)\right] \tag{19}$$

where $\beta_R = \sigma_{\ln EDP|LM}$. Like Eqs. (6) and (8), Eq. (19) is comprised of two parts. The first describes the variation of λ_{EDP} with *EDP* based on the mean *IM* and median *IM*–*LM* and *LM*–*EDP* relationships. The second part accounts for uncertainty in the prediction of *LM* given *IM* and of *EDP* given *LM*.

7.2.1 Displacement capacity exceedance rate

The displacement capacity is typically taken as the maximum displacement associated with some limit state. Taking the allowable displacement, which is usually estimated by approximate means, to be uncertain, the hazard curve for the limit state, $LS = EDP > C = c$, is

$$\lambda_{LS} = \int_0^\infty \lambda_{EDP}(c) f_C(c) dc \tag{20}$$

which can be evaluated numerically. If the capacity is lognormally distributed, the closed-form expression of Eq. (19) can be used to show that

$$\lambda_{EDP}(edp) = k_0 \left[\frac{1}{a} \left(\frac{\hat{C}}{d} \right)^{1/e} \right]^{-k/b} \exp \left[\frac{k^2}{2b^2 e^2} \left(e\beta_L^2 + \beta_R^2 + \beta_C^2 \right) \right] \tag{21}$$

where $\hat{C}$ is the median displacement capacity. This closed-form expression can be used to derive expressions for the *EDP*s corresponding to a given mean annual rate of exceedance for the cases of (a) zero uncertainty in load, response, and capacity, (b) uncertain load and response but no uncertainty in capacity, and (c) uncertain load, response, and capacity. These *EDP* values can be written as

$$EDP_0 = d \left(\frac{\lambda_{EDP}}{k_0 a^{k/b}} \right)^{-be/k} \tag{22}$$

$$EDP_{LR} = d \left(\frac{\lambda_{EDP}}{k_0 a^{k/b}} \right)^{-be/k} \exp \left[\frac{k}{2be} \left(e\beta_L^2 + \beta_R^2 \right) \right] \tag{23}$$

$$EDP_{LRC} = d \left(\frac{\lambda_{EDP}}{k_0 a^{k/b}} \right)^{-be/k} \exp \left[\frac{k}{2be} \left(e\beta_L^2 + \beta_R^2 + \beta_C^2 \right) \right] \tag{24}$$

A similar approach to that used for the force-based load and resistance factors can be applied to the development of a displacement-based LRFD-like design framework. To distinguish the displacement-based case from the force-based case, the factors developed here will be described as demand and capacity factors.

7.2.2 Demand and capacity factors

With the goal of relating the response computed deterministically to that computed considering uncertainties in load, demand, and capacity, demand and capacity factors can be defined as

$$DF = \frac{EDP_{LR}}{EDP_0} \tag{25a}$$

and

$$CF = \frac{EDP_{LR}}{EDP_{LRC}} \tag{25b}$$

A design based on the requirement that

$$DF \cdot \hat{D} \le CF \cdot \hat{C} \tag{26}$$

where $\hat{D}$ is the median value of *EDP* and $\hat{C}$ is the median capacity, would correspond to an annual rate of limit state exceedance equal to that corresponding to $\hat{D}$ and $\hat{C}$.

The resulting demand factor is

$$DF = \exp \left[\frac{1}{2} \frac{k}{be} (e^2 \beta_L^2 + \beta_R^2) \right], \tag{27a}$$

and the capacity factor is

$$CF = \exp \left[-\frac{1}{2} \frac{k}{be} \beta_C^2 \right] \tag{27b}$$

Note that, under the assumptions of the closed-form solution, the demand and capacity factors are constants, i.e., they do not vary with return period.

7.3 Application to pile foundation design

The force- and displacement-based frameworks described in the preceding section were applied to the design of pile groups in non-liquefiable soils. A decoupled approach to the estimation of pile group loads and displacements was used; such an approach can result in inaccurate loading histories for specific structures when loads are high enough to produce extremely high levels of nonlinearity, but it provides a computationally feasible approach for a general investigation.

Pile group loading histories were obtained by three-dimensional analyses of a lumped-mass structure supported by a pile-supported footing excited by three components of input motion. The motions were applied through spring/dashpot elements whose impedances where obtained from DYNA4 (Novak and Aboui-Ella 1978) analyses. An iterative procedure was used to obtain displacement/rotation-compatible foundation impedances. The structural analyses, which were performed using OpenSees (http://opensees.berkeley.edu/OpenSees/copyright.php), yielded loading histories in the x-, y-, and z-directions, and histories of overturning moments about the x- and y-axes. A total of 50 input motions representing a wide range of magnitude-distance scenarios were applied to the model.

The resulting loading histories were then applied to a three-dimensional OpenSees model of a pile foundation. The OpenSees model represented pile–soil interaction using $p-y$, $t-z$, and $Q-z$ elements based on the model of Shin (2007), which had been shown capable of accurately modeling full-scale static load tests and dynamic centrifuge model tests. Different pile group configurations in different soil profiles were analyzed with each of the 50 input motions resulting in a large database of computed pile group responses. The computed responses showed a high level of dispersion for different pile groups, configurations, soil profiles, and input motions. The dispersion was markedly reduced, however, by normalizing loads and displacement by reference values of each. The reference loads were taken as those corresponding to common notions of "failure"—the vertical load obtained by the Davisson (1973) load test interpretation procedure, the lateral load that produced pile head displacement equal to 10 % of the pile diameter under monotonic loading, and the overturning moment that produced the Davisson reference load in the outermost piles. The reference displacements were taken as those corresponding to the reference loads.

Regression analyses were performed to relate normalized displacements to normalized loads; it was observed that all five components of displacement were influenced by all five components of load. As an example, the normalized lateral displacement in the x-direction was given by

$$\ln u_n = 0.191 + 0.364 \ln Q_n + 0.990 V_{xn} - 0.320 V_{yn} + 0.796 \ln(M_{xn} + M_{yn}) \quad (28)$$

where Q_n, V_{xn}, V_{yn}, M_{xn}, and M_{yn} are the normalized loads; the computed dispersion for this relationship, $\sigma_{\ln u_n} = 0.749$, is quite high.

A computer program was developed to allow determination of both load- and displacement-based design factors for pile groups. The user defines the pile group and soil conditions and the (uncertain) static loads acting on the foundation. The program assumes that the relationship between structural loads and ground motion intensity measures have been established by means of structural response analyses—the median *IM–LM* relationship is assumed to be segmentally linear in log–log space with lognormal dispersion, β_L, and user-defined load correlation. A series of Monte Carlo simulations accounts for uncertainties in static loads,
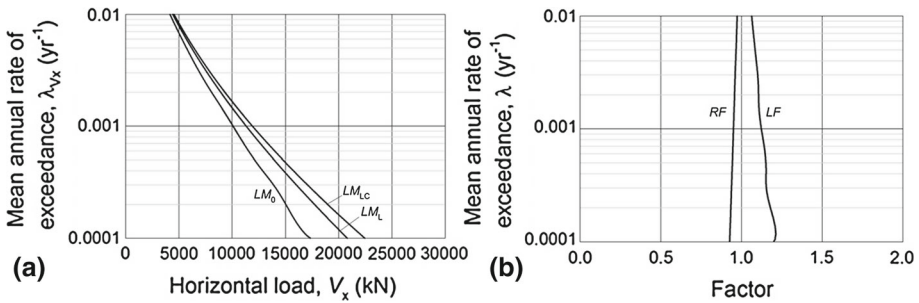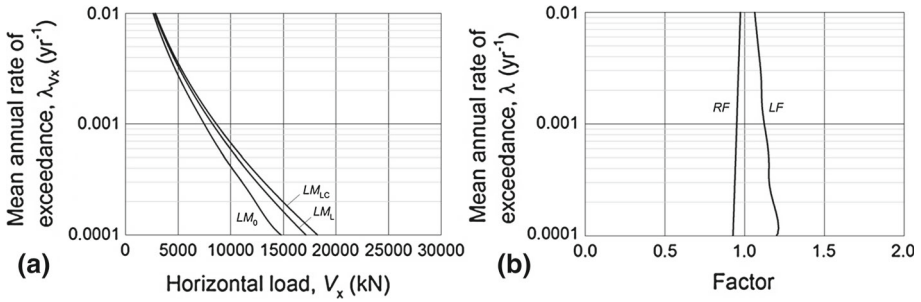
Fig. 5 San Francisco site results: **a** horizontal load hazard curves, and **b** load and resistance factors

reference loads, dynamic loads (including their correlation structure), and dynamic deformations (displacements and rotations) over all five components of loading to define probabilistic *LM–EDP* vector relationships. These relationships are then used, integrating over all *IM* levels and all components of five-dimensional *LM* space to develop the *EDP* hazard curves from which demand and capacity factors can be obtained.

Consider the case of a 5×5 group of 60-cm diameter steel pipe piles embedded in a uniform profile of medium dense sand. The pile group supports a bridge with a constant fundamental period of 0.5 s that imposes a static vertical load of 40,000 kN, static lateral loads of 10,000 and 15,000 kN in the *x*- and *y*-directions, and static overturning moments of 30,000 and 20,000 kN-m about the *x*- and *y*-axes. If the bridge is located in different seismic environments, its *LM* and *EDP* hazard curves, and therefore its design factors, may be different. Figure 5 shows *LM* hazard curves and corresponding load and resistance factors for the pile foundation is located in San Francisco, California assuming $\beta_L = 0.2$ for all *LM* vector components and $\beta_C = 0.3$ for all capacity vector components. While the three *LM* hazard curves appear to be very smooth, the spline function used to interpolate between the six periods of the USGS spectral acceleration hazard curve introduces a slight variation that becomes more apparent when their ratios are computed for the load and resistance factors. It is readily apparent, however, that the load factors increase and resistance factors decrease with increasing return period. For the conditions used in this example, the variability of these factors with return period results from the fact that the hazard curves are not of power law form. Figure 6 shows corresponding results for the same foundation assumed to be located in Seattle, Washington. Although the *LM* hazard curves are different than those of San Francisco, properly reflecting San Francisco's higher seismicity levels, the load and resistance factors are much more similar. In both cases, neither the load and resistance factors are significantly different than unity due to the relatively good accuracy with which loads in a single-mass structure can be computed given first-mode spectral acceleration and the relatively modest uncertainty in load capacity.

The design conditions for the pile group in San Francisco and Seattle can also be examined from a displacement-based point of view. Displacements are well known to be considerably more difficult to compute than forces. As a result, the values of $\beta_R = \sigma_{\ln LM|IM}$ are much higher than the values of $\beta_L = \sigma_{\ln LM|IM}$. Furthermore, the calculation of EDP_{LR} includes the effects of uncertainties in both $LM|IM$ and $EDP|LM$. Figure 7 shows *x*-direction displacement hazard curves and displacement demand and capacity factors for the pile group in San Francisco. The demand and capacity factors can be seen in Fig. 7a to be very widely spaced. The zero-uncertainty horizontal displacement increases with increasing return period, but at a relatively slow rate. Due to the high levels of uncertainty in response

Fig. 6 Seattle site results: **a** horizontal load hazard curves, and **b** load and resistance factors
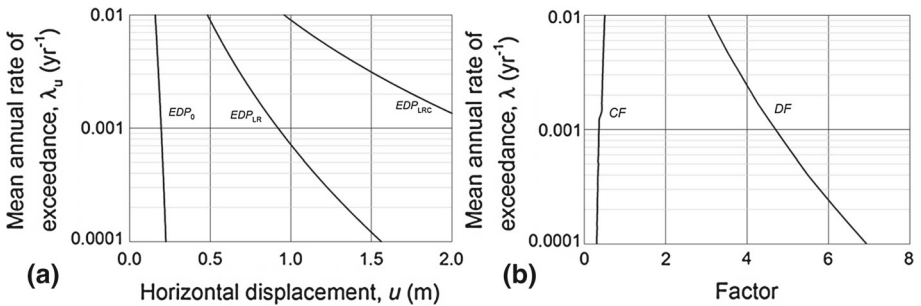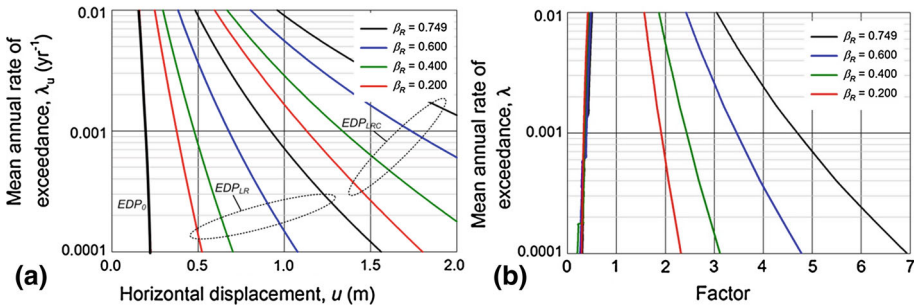

Fig. 7 San Francisco site results: **a** horizontal displacement hazard curves, and **b** capacity and demand factors
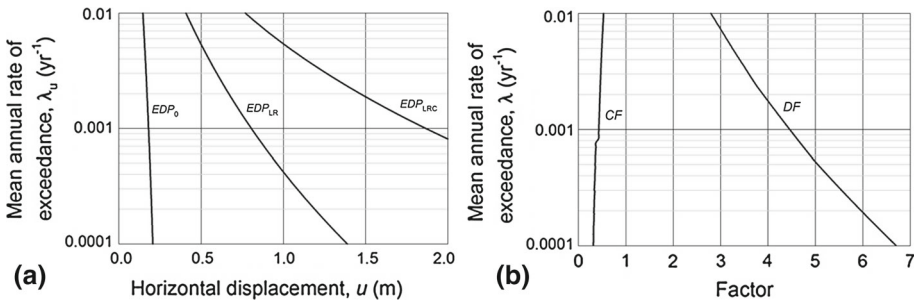
Fig. 8 Seattle site results: **a** horizontal displacement hazard curves, and **b** capacity and demand factors

($\beta_L = 0.2$; $\beta_R = 0.749$), the value of EDP_{LR} at a particular return period is much larger than EDP_0, particularly at long return periods. Assuming that the uncertainty in allowable horizontal displacement (i.e., displacement capacity) is similar to that estimated for buildings ($\beta_C = 0.8$) by Bird et al. (2005), the curve for displacement considering uncertainties in load, displacement, and capacity, EDP_{LRC}, is larger yet. Figure 7b shows the corresponding demand and capacity factors for horizontal displacement. In contrast to the force-based load and resistance factors, the displacement-based demand and capacity factors are far from unity. Demand factors vary from approximately 3–7 and capacity factors from about 0.5 to 0.2. The corresponding results for Seattle are shown in Fig. 8. Again, the hazard curves for Seattle and San Francisco are significantly different, but the capacity and demand factors are similar.

Fig. 9 San Francisco results with different levels of response uncertainty: **a** horizontal displacement hazard curves, and **b** capacity and demand factors (demand factors are >1.0 and capacity factors are <1.0)

As previously discussed, uncertainty tends to amplify the level of response at a given hazard level, or return period. In the case of a displacement-based capacity and demand factor design framework, uncertainty leads to high demand factors and low capacity factors. Reducing these uncertainties can lead to lower demand factors and higher capacity factors. Figure 9 shows, for example, the effects of reduced response uncertainty on horizontal displacement hazard curves and on the resulting capacity and demand factors. As shown in Fig. 9a, lower values of β_R lead to lower values of EDP_{LR} at a particular hazard level, and the lower values of EDP_{LR} lead in turn to lower values of EDP_{LRC}. These changes result in significantly lower demand factors (Fig. 9b), while negligibly affecting the capacity factors.

The dominant role of uncertainty in probabilistically-based performance-based design becomes even more apparent when design is implemented at the response level. Reduction of uncertainty is an important and efficient avenue for the more economical design of soil-foundation-structure systems.

8 Summary and conclusions

The performance of structures during earthquakes can be characterized in terms of response, damage, and loss. Owners, operators, and other decision-makers are primarily interested in managing risk, so the accurate estimation of potential losses remains the ultimate goal of performance-based design procedures.

The application of performance-based concepts to seismic evaluation and design has increased significantly in recent years. While performance-based design can be accomplished in a number of different ways, its use in practice to date has nearly always focused on response measures such as displacements as indicators of performance. Such an approach requires the inference of damage and loss from displacement. The inference of damage and loss is usually done in an informal manner, which contributes to the uncertainty in losses. In practice, it is usually implemented using a discrete number of ground motion hazard levels, or return periods. Integral hazard level frameworks, such as that proposed by PEER, are also available. Nevertheless, the adoption of performance-based design has led to greater flexibility in design, more appropriate expected performance in large and small earthquakes, and improved interaction between design professionals.

A fully probabilistic implementation of performance-based design requires a voluminous number of calculations that can be very time-consuming, particularly for complex soil-foundation-structure systems in areas subjected to strong earthquake shaking. For large and

complex projects, the full procedure may be too time-consuming for application during all design iterations; in such cases, it may be applied to the final design to evaluate the extent to which it satisfies all performance objectives. For the more routine design of typical structures, a simpler design procedure that provides the benefits of a probabilistic performance-based design framework without requiring the user to perform multiple or complex probabilistic analyses is desirable.

Both force- and displacement-based design approaches can be implemented in a manner consistent with the PEER performance framework. Both require characterization of ground motion hazards by means of a probabilistic seismic hazard analysis. In the force-based approach, probabilistic representations of force given ground motion and of capacity are required. By combining force fragility functions with ground motion hazard curves, force hazard curves with different uncertainty components can be computed. Load and resistance factors can then be defined in terms of ratios of loads at consistent return periods. With this approach, a designer must determine the median load from deterministic analyses (with a sufficient number of input motions to establish the median) and best-estimate properties. Using load and resistance factors associated with a design limit state return period, the provision of a factored capacity that exceeds the factored load produces a design with the desired level of performance.

The force-based approach has been extended to a displacement-based approach in which displacement demand and capacity factors can be applied to median displacements and allowable displacements (displacement capacities) to produce a design with a desired return period for exceedance of allowable displacement. The relatively high levels of uncertainty in displacement prediction and displacement capacity can lead to demand and capacity factors that differ significantly from unity.

The reduction of uncertainty by the acquisition of extensive subsurface data and the careful performance and interpretation of sophisticated analyses can lead to more economical design for a given hazard level. Research and new tools and techniques for ground motion and site characterization, and soil-foundation-structure interaction analysis will help produce more reliable and efficient structures and facilities.

References

Algermissen ST, Perkins DM (1976) A probabilistic estimate of maximum acceleration in rock in the contiguous United States, US Geological Survey Open-File Report 76–416, 45 pp

Applied Technology Council (1978) Tentative provisions for the development of seismic regulations for buildings, ATC 3–06, NSF 78–8. Applied Technology Council, Redwood City

Bartlett SF, Youd TL (1992) Empirical analysis of horizontal ground displacement generated by liquefaction-induced lateral spread, Technical Report NCEER-92-0021. National Center for Earthquake Engineering Research, Buffalo, NY

Biondi G, Maugeri M, Cascone E (2009) Performance-based pseudo-static analysis of gravity retaining walls. In: Kokusho T, Tsukamota Y, Yoshimine M (eds) Performance-based design in earthquake geotechnical engineering: from case history to practice. Taylor and Francis, London, pp 571–580

Bird JF, Crowley H, Pinho R, Bommer JJ (2005) Assessment of building response to liquefaction-induced differential ground deformation. Bull N Z Soc Earthq Eng 38(4):215–234

Bray JD, Travasarou T (2007) Simplified procedure for estimating earthquake-induced deviatoric slope displacements. J Geotech Geoenviron Eng ASCE 133(4):381–392

Chatzigogos CT, Figini R, Pecker A, Salencon J (2011) A macroelement formulation for shallow foundations on cohesive and frictional soils. Int J Numer Anal Methods Geomech 35:902–931

Cornell CA (1968) Engineering seismic risk analysis. Bull Seismol Soc Am 58:1583–1606

Cornell CA, Krawinkler H (2000) Progress and challenges in seismic performance assessment. PEER News, April 1–3

Cornell CA, Jalayer F, Hamburger RO, Foutch DA (2002) Probabilistic basis for 2000 SAC Federal Emergency Management Agency steel moment frame guidelines. J Struct Eng ASCE 128(4):526–533

Correia AA, Pecker A, Kramer SL, Pinho R (2012) A pile-head macro-element approach to seismic design of extended pile-shaft-supported bridges. In: Proceedingsof the second international conference on performance-based design in geotechnical earthquake engineering, Paper 7.03, Taormina, Italy, 12 pp

Cremer C, Pecker A, Davenne L (2001) Cyclic macroelement for soil-structure interaction: material and geometric nonlinearities. Int J Numer Anal Methods Geomech 25:1257–1284

Cremer C, Pecker A, Davenne L (2002) Modeling of nonlinear dynamic behavior of a shallow strip foundation with macroelement. J Earthq Eng 6(2):175–211

Cubrinovsky M, Bradley BA (2009) Evaluation of seismic performance of geotechnical structures. In: Kokusho T, Tsukamota Y, Yoshimine M (eds) Performance-based design in earthquake geotechnical engineering: from case history to practice. Taylor and Francis, London, pp 121–136

Davisson MT (1973) High capacity piles. In: Proceedings of a lecture series on innovations in foundation construction. Illinois Section ASCE, Chicago

Deierlein GG, Krawinkler H, Cornell CA (2003) A framework for performance-based earthquake engineering. In: Proceedings of the 2003 Pacific conference on earthquake engineering

Department of Energy (1994) Natural phenomena hazards design and evaluation criteria for Department of Energy Facilities, DOE-STD-1020-94. US Department of Energy, Washington, DC

Iai S, Tobita T, Tamari Y (2008) Seismic performance and design of port structures. In: Proceedings of the geotechnical earthquake engineering and soil dynamics IV. ASCE, Sacramento, CA

Jalayer F (2003) Direct probabilistic seismic analysis: implementing non-linear dynamic assessments. Ph.D. dissertation. Stanford University, Stanford, CA

Juang C-H, Li DK, Fang SY, Liu Z, Khor H (2008) Simplified procedure for developing joint distribution of a_{max} and M_w for probabilistic liquefaction hazard analysis. J Geotech Geoenviron Eng ASCE 134(8):1050–1058

Kramer SL, Mayfield RT (2005) Performance-based liquefaction hazard evaluation. In: Proceedings of the GeoFrontiers 2005. ASCE, Austin, AX

Kramer SL, Mayfield RT, Huang Y-M (2006) Performance-based liquefaction potential: a step toward more uniform design requirements. In: Proceedings of the US-Japan workshop on seismic design of bridges. Bellevue, WA

Kramer SL, Mayfield RT (2007) The return period of liquefaction. J Geotech Geoenviron Eng ASCE 133(7):1–12

Kramer SL (2011) Performance-based design in geotechnical earthquake engineering practice. In: Proceedings of the 5th international conference on earthquake geotechnical engineering on invited state-of-the-art paper. Santiago, Chile

Ledezma C, Bray JD (2010) Probabilistic performance-based procedure to evaluate pile foundations at sites with liquefaction-induced lateral displacement. J Geotech Geoenviron Eng ASCE 136(3):464–476

Luco N, Cornell CA (1998) Seismic drift demands for two SMRF structures with brittle connections, structural engineering world wide 1998. Elsevier, Oxford

Makdisi FI, Seed HB (1978) Simplified procedure for estimating dam and embankment earthquake induced deformations. J Geotech Eng Div ASCE 104(GT7):849–867

Marrone J, Ostadan F, Youngs R, Itemizer J (2003) Probabilistic liquefaction hazard evaluation: method and application. In: Proceedings of the 17th international conference structural mechanics in reactor technology (Smart 17). Prague, Czech Republic, Paper No. M02–1

Mononobe N, Matsuo H (1929) On the determination of earth pressures during earthquakes. In: Proceedings of the world engineering congress, vol 9

Newmark N (1965) Effects of earthquakes on dams and embankments. Geotechnique 15(2):139–160

Nova R, Montrasio L (1991) Settlements of shallow foundations on sand. Geotechnique 41(2):243–256

Novak M, Aboui-Ella F (1978) Impedance functions of piles in layered media. J Geotech Eng ASCE 104(EM3):643–661

Okabe S (1926) General theory of earth pressures. J Jpn Soc Civil Eng 12(1)

Paolucci R (1997) Simplified evaluation of earthquake-induced permanent displacements of shallow foundations. J Earthq Eng 1(3):563–579

Rathje EM, Saygili G (2008) Probabilistic seismic hazard analysis for the sliding displacement of slopes: scalar and vector approaches. J Geotech Geoenviron Eng ASCE 134(6):804–814

Richards R, Elms D (1979) Seismic behavior of gravity retaining walls. J Geotech Eng Div ASCE 105(GT4):449–464

Rix GJ (2009) Risk measures in design of geotechnical structures. In: Kokusho T, Tsukamoto Y, Yoshimine M (eds) Performance-based design in earthquake geotechnical engineering: from case history to practice. CRC Press, Balkema, Leiden, pp 269–272

SEAOC (1995) Vision 2000: performance-based seismic engineering of buildings. Structural Engineers Association of California, Sacramento, CA

Shin H-S (2007) Numerical modeling of a bridge system and its application for performance-based earthquake engineering. Ph.D. Thesis. University of Washington, Seattle, WA

Sunasaka Y, Niihara Y, Tashiro S, Asanuma T, Miyata M, Noguchi T (2009) Performance-based seismic design of structures connecting reclaimed island and piled-elevated platform in Tokyo International Airport re-expansion project. In: Kokusho T, Tsukamota Y, Yoshimine M (eds) Performance-based design in earthquake geotechnical engineering: from case history to practice. Taylor and Francis, London, pp 1719–1727

Towhata I, Yoshida I, Ishihara Y, Suzuki S, Sato M, Ueda T (2009) On design of expressway embankment in seismically active area with emphasis on life cycle cost. Soils Found 49(6):871–882

Travasarou T, Bray JB, Der Kiureghian A (2004) A probabilistic methodology for assessing seismic slope displacements. In: Proceedings of the 13th world conference on earthquake engineering, Paper 2326. Vancouver

Youd TL, Hansen CM, Bartlett SF (2002) Revised multilinear regression equations for prediction of lateral spread displacement. J Geotech Geoenviron Eng ASCE 128(12):1007–1017